

ADVANCED REACTOR PASSIVE SYSTEM RELIABILITY DEMONSTRATION ANALYSIS FOR AN EXTERNAL EVENT

Matthew D. Bucknor¹, David Grabaskas¹, Acacia J. Brunett¹, Austin Grelle¹

¹Argonne National Laboratory, Argonne, IL 60439, mbucknor@anl.gov

Many advanced reactor designs rely on passive systems to fulfill safety functions during accident sequences. These systems depend heavily on boundary conditions to induce a motive force, meaning the system can fail to operate as intended due to deviations in boundary conditions, rather than as the result of physical failures. Furthermore, passive systems may operate in intermediate or degraded modes. These factors make passive system operation difficult to characterize within a traditional probabilistic framework that only recognizes discrete operating modes and does not allow for the explicit consideration of time-dependent boundary conditions. Argonne National Laboratory has been examining various methodologies for assessing passive system reliability within a probabilistic risk assessment for a station blackout event at an advanced small modular reactor. This paper provides an overview of a passive system reliability demonstration analysis for an external event. Centering on an earthquake with the possibility of site flooding, the analysis focuses on the behavior of the passive reactor cavity cooling system following potential physical damage and system flooding. The assessment approach seeks to combine mechanistic and simulation-based methods to leverage the benefits of the simulation-based approach without the need to substantially deviate from conventional probabilistic risk assessment techniques. While this study is presented as only an example analysis, the results appear to demonstrate a high level of reliability for the reactor cavity cooling system (and the reactor system in general) to the postulated transient event.

I. INTRODUCTION

Advanced reactor designers continue to strive for increased resilience and reliability through the use of passive safety systems. Removal of active components and dependency on operator intervention tends to increase the reliability of these types of systems as significant failure modes are removed. However, integration of the failure of these systems into a traditional risk assessment framework can be challenging, as conventional assessment techniques, which focus on active failures, cannot be applied directly. Additionally, historical U.S. licensing efforts have not included risk-informed treatment of passive systems, largely due to the omission of passive safety systems from legacy designs. For the future licensing of advanced reactor designs to progress, a path forward must be identified for the inclusion of passive systems in a risk-informed regulatory framework. For these reasons, this effort focuses on the development and demonstration of a reliability analysis methodology for passive systems that addresses the challenges of passive system reliability assessments and its inclusion in a regulatory framework.

The goal of this project is to provide a path forward for advanced reactor vendors who will soon be approaching regulatory bodies and seeking to demonstrate the reliability of the passive safety systems incorporated into their plants. As indicated in the *Proposed Risk Management Regulatory Framework* (Ref. 1), published in 2012, the Nuclear Regulatory Commission (NRC) foresees a future regulatory environment that combines both traditional deterministic analysis and probabilistic risk assessments (PRAs). A key facet of this plan is the reliance on mechanistic reliability analyses to forgo some of the conservative assumptions of past analyses. This presents advanced reactor designers with an opportunity to realistically demonstrate plant performance, but also requires realistic modeling of all safety related plant systems, including passive systems.

II. EXTERNAL EVENT DEMONSTRATION ANALYSIS

The approach utilized for the assessment of passive system reliability in this work is a variation of the Reliability Method for Passive Systems (RMPS) (Ref. 2). The RMPS provides a rigorous and structured approach to the assessment of passive system reliability. However, for the analysis conducted here, the RMPS procedure has been modified slightly to include the advanced uncertainty assessment and propagation techniques that were explored in previous work (Ref. 3). These techniques will be discussed in greater detail in Section II.F. Figure 1 shows the methodology roadmap utilized for this external event analysis.

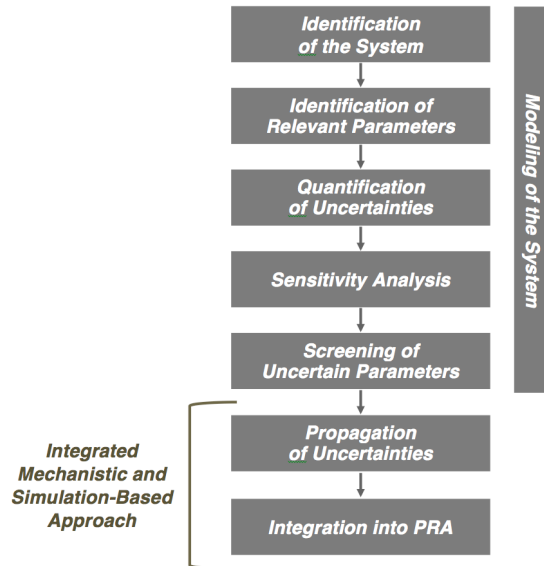


Fig. 1. Demonstration Analysis Methodology.

The methodology is similar to the process utilized for the station blackout analysis in (Ref. 3) with initial steps focused on the identification of the system of interest, and establishment of success/failure criteria. This is followed by the identification of relevant parameters, including quantification and screening of the parameters. In parallel, a best-estimate (BE) model of the system of interest is created, which is used in the penultimate step of uncertainty propagation. As will be described in Section II.F, unlike the analysis performed in (Ref. 3), where two uncertainty propagation and PRA integration techniques were assessed (a mechanistic method and a simulation-based method), a single combined methodology is utilized that seeks to leverage the best features of both of the previously tested methods.

II.A. Identification of System

The first step of the analysis process is the identification of the system and scenario. The transient analyzed here is an extreme external event at a small, pool-type, metal-fuel, sodium-cooled fast reactor (SFR). Following the accident at the Fukushima Daiichi nuclear power plant, external events are receiving greater attention by both the regulator and industry. In particular, the use of passive systems is seen as one possible strategy for mitigating the effects of such an event. However, combining the difficulties of assessing passive system reliability with the challenges of an extreme external event can make risk analyses problematic. Providing a pathway to address such events was a key motivation for the current work.

The SFR design, seen in Figure 2 with design characteristics listed in Table I, was used for the external event assessment. The plant has an intermediate sodium loop that transports heat from the primary sodium to the secondary side, which contains a steam generator and turbine. Within the reactor vessel, the hot sodium leaving the reactor core must pass through the intermediate heat exchanger (IHX) before reaching the cold pool region.

The IHX and the associated secondary coolant are the primary heat removal pathways for the primary sodium system during normal operation and off-normal transients. However, in the event of loss of secondary side heat removal capabilities, or the loss of intermediate loop pumping power, heat must be removed through the Reactor Cavity Cooling System (RCCS). The RCCS is based on the design of a similar system utilized by the General Atomics Modular High Temperature Gas cooled Reactor (GA-MHTGR) (Ref. 4). The decision to analyze an RCCS was motivated by the availability of the Natural convection Shutdown heat removal Test Facility (NSTF) at Argonne. The facility, which is configured as a one half-scale RCCS, is currently performing ongoing passive cooling experiments; the results of these ongoing tests are used to validate the overall trends of the system models utilized for this demonstration problem.

The RCCS, which is shown in Figure 3 (Ref. 4) (Ref. 5), uses natural convection to drive air from the environment through cold downcomers and into a lower plenum. The air then flows through hot riser tubes that surround the reactor guard vessel and line the inner wall of the concrete containment vessel. Heat from the guard vessel is transferred to the air in the hot riser tubes through a combination of radiation and convection; in this design, heat is ultimately rejected to the environment. The RCCS is designed to remove decay heat, but because it is completely passive (no baffle or damper operation is required), it also functions during normal reactor operation.

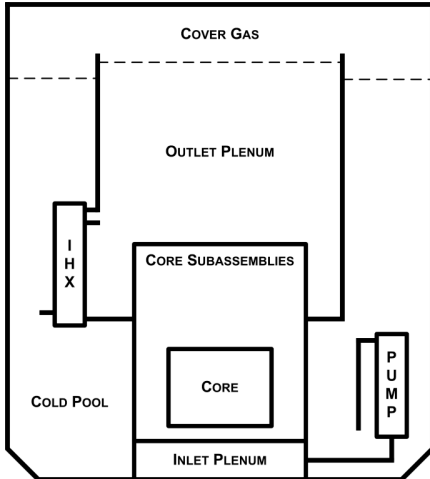


TABLE I. Design Characteristics of Demonstration SFR.

Characteristics	
Power rating	250 MWth/100 MWe
Primary coolant	Sodium
Primary system type	Pool
Fuel type	Metallic
Primary coolant flow rate	~ 1270 kg/s
Coolant pump type	Electromagnetic
Number of coolant pumps	4
Primary vessel height	10 m
Core inlet temperature	~ 400°C
Core outlet temperature	~ 550°C

Fig. 2. Schematic of Primary System of Demonstration SFR.

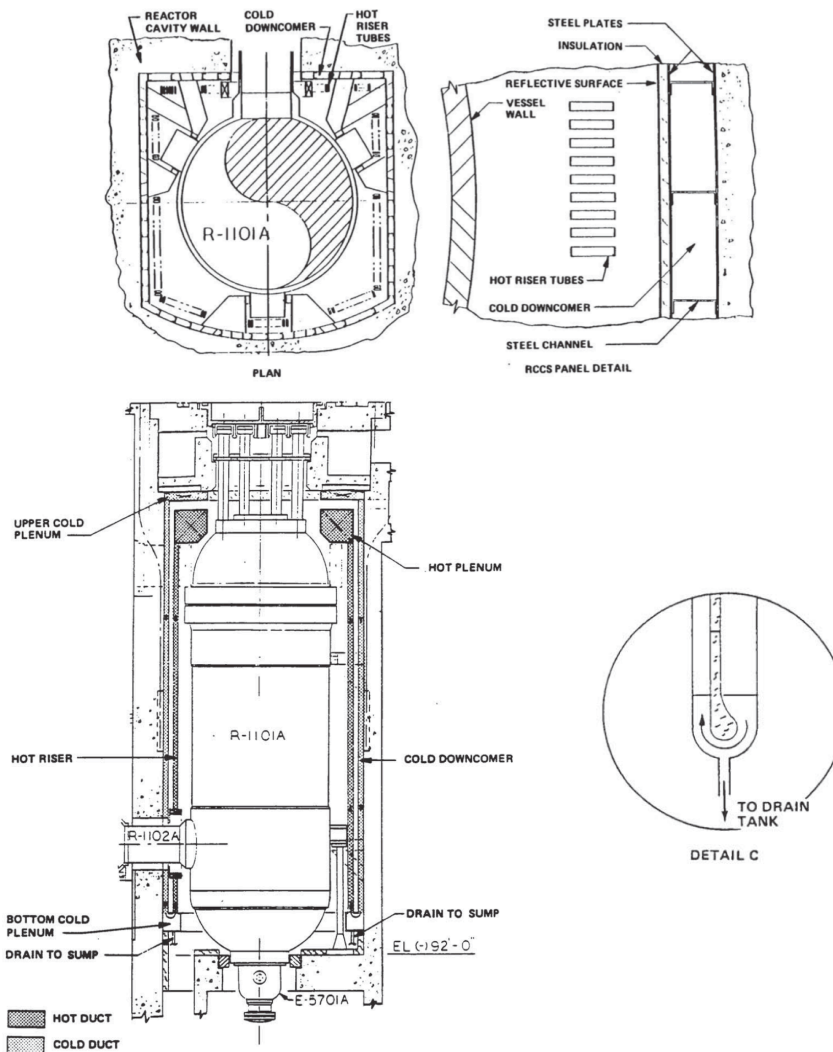


Fig. 3. GA-MHTGR Cavity and RCCS Layout including Detail of Sump Drain (Ref. 4) (Ref. 5).

II.B. Description of Scenario

An extreme external event was analyzed for the passive system reliability demonstration analysis. In this case, an earthquake, with the possibility of subsequent tsunami/flooding, was chosen due to its challenging nature and recent attention from the regulator as a result of the events at Fukushima Daiichi. In the scenario, a station blackout occurs following the earthquake, and the possibility of site flooding occurs shortly thereafter. An event tree was generated using SAPHIRE (Ref. 6) for the analysis, and is shown in Figure 4.

Rather than creating separate event trees for a multitude of earthquakes sizes, the event tree includes multiple seismic intensity ranges (with only one seismic intensity range (0.06 – 0.2g) fully shown in Figure 4; the remaining seismic intensity branches have identical sequences). However, the probabilities of some top events in the event tree vary depending on the seismic intensity range. The earthquake event tree is based largely on the HTGR PRA earthquake event tree (Ref. 7), with several top events taken from the PRISM SFR PRA (Ref. 8).

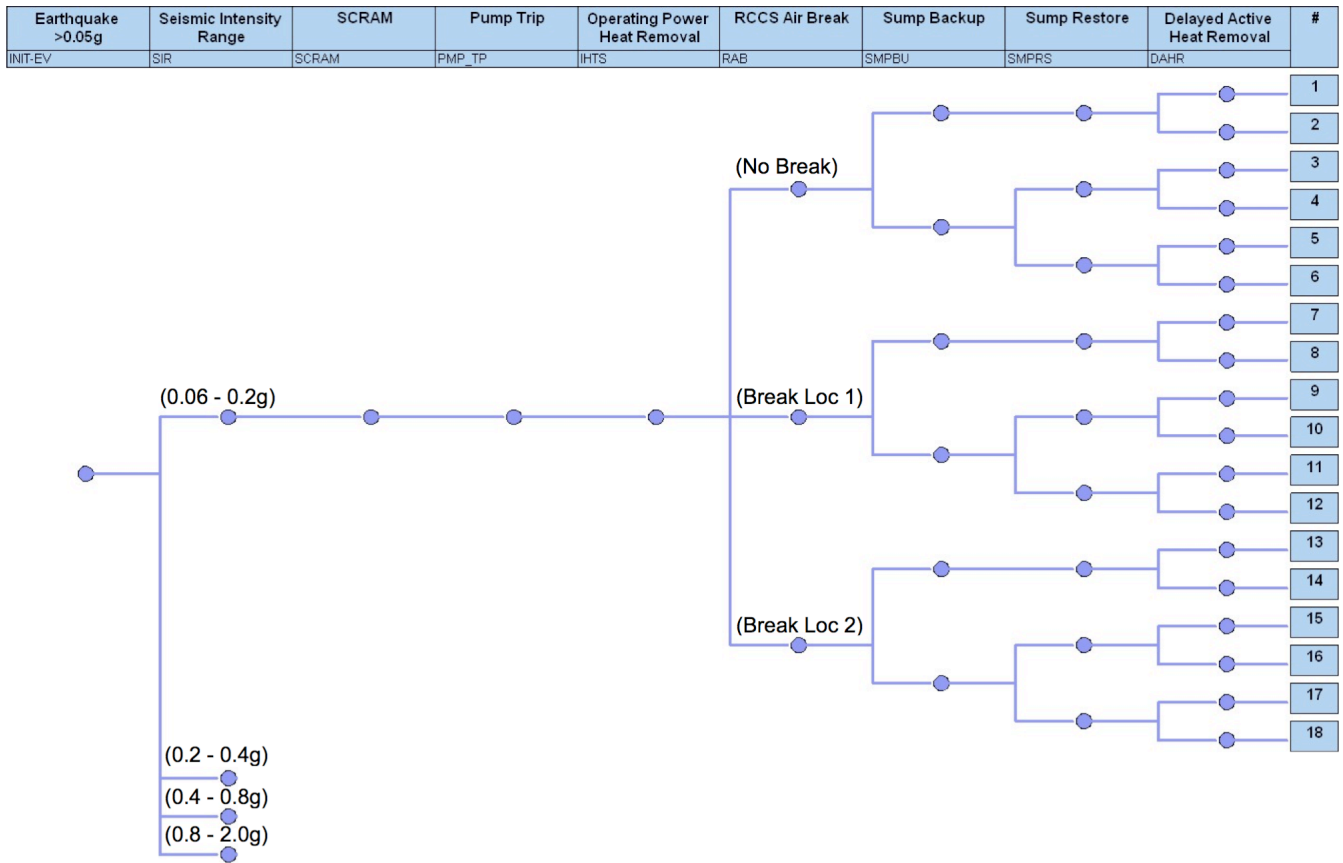


Fig. 4. Earthquake Event Tree.

II.B.1. Initiating Event: Earthquake

The initiating event is an earthquake with peak ground acceleration above 0.05g. As stated in the HTGR PRA (Ref. 7), “a 0.06g delimitator has been introduced to differentiate between "earthquakes" and normal seismic background in which no damage to typical commercial or residential structures is expected.” The seismic curve used here, shown in Figure 5, was utilized in the HTGR PRA (Ref. 7) and was taken from the Watt’s Bar site in Tennessee. Based on this seismic curve, the frequency of an earthquake with a magnitude greater than 0.05g is approximately 5×10^{-3} per year.

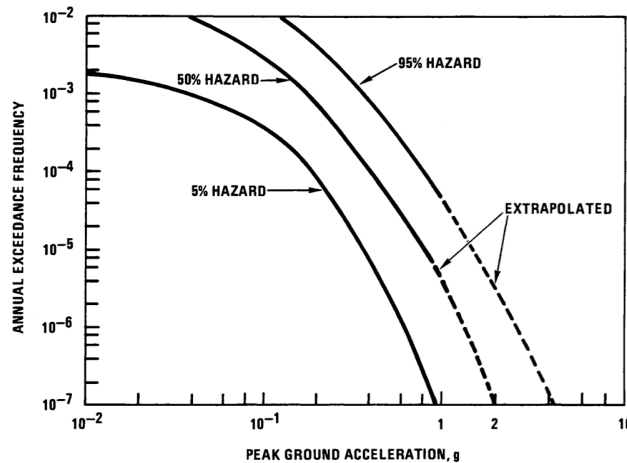


Fig. 5. HTGR Seismic Curve (Ref. 7).

II.B.2. Top Event: Seismic Intensity Range

The initiating event simply states the occurrence of an earthquake with peak ground acceleration above 0.05g. However, to accurately gauge the plant response to an earthquake, greater discretization is necessary. Therefore, the next top event in the event tree is the seismic intensity range, which specifies a more precise peak ground acceleration range. This event is non-binary, with four possible seismic intensity ranges, shown in Table II. Probabilities for each seismic intensity range were taken from the HTGR PRA (Ref. 7), again using the Watt's Bar seismic curve. The number of intensity ranges and their bounds were selected based on the estimated minimum seismic intensity that could impact important safety systems of the plant.

TABLE II. Seismic Intensity Range Probabilities.

Seismic Intensity Range	Probability
0.06 – 0.2g	8.88×10^{-1}
0.2g – 0.4g	9.00×10^{-2}
0.4 – 0.8g	2.00×10^{-2}
0.8 – 2.0g	2.00×10^{-3}

II.B.3. Top Event: SCRAM

For the earthquake analysis conducted here, it was assumed that the reactor protection system operated successfully during and following the earthquake, and that the plant has shutdown successfully (reactor SCRAM probability equals unity). This assumption was made for several reasons. First, analyzing only protected scenarios helped limit the scope of the passive system reliability demonstration analysis. As seen in Figure 4, even with only protected sequences, the earthquake event tree will have 72 unique end states. Adding unprotected sequences would have caused this number to increase significantly, and a detailed analysis of all sequences would not have been feasible within the limits of the current project. Second, during unprotected accidents, metal fuel, pool-type SFRs rely heavily on inherent reactivity feedback to lower reactor power. However, during seismic events, the motion of the primary sodium, along with the motion of control rod drivelines and core fuel assemblies, can make the accurate prediction of inherent reactivity feedback difficult. As the focus of the analysis is on the performance of the passive RCCS, and not inherent reactivity feedback (although they are also an important passive phenomena), the decision was made to only analyze protected sequences.

II.B.4. Top Event: Pump Trip

It is assumed that for all four of the seismic intensity ranges examined, offsite power is lost due to the earthquake. In turn, all primary electromagnetic (EM) pumps lose power and trip with probability equal to unity (as there is no emergency diesel in the SFR plant configuration analyzed here). As will be described in Section II.E, the effect of successful pump coastdown, which is provided by a separate synchronous machine for EM pumps, was evaluated through sensitivity analyses

and found to have no impact for the protected sequences analyzed. Therefore, scenarios for different number of pump coastdown failures are not represented in the earthquake event tree.

II.B.5. Top Event: Operating Power Heat Removal

Since offsite power is lost as a result of the earthquake, the generator and turbine on the secondary side of the balance of plant also trip with probability equal to unity. This results in the RCCS being the main heat removal pathway for the duration of the scenario.

II.B.6. Top Event: RCCS Air Break

The next top event in the event tree examines the possibility of damage (a duct wall break) to the RCCS due to seismic motion. The possible RCCS damage scenarios are: no break, a duct wall break at location 1, or a duct wall break at location 2. Details of break locations 1 and 2 are discussed in more detail in Section II.C. The probability of an RCCS duct wall break was found using the RCCS fragility curve given in the HTGR PRA (Ref. 7), which is shown in Table III. Then, using the peak ground acceleration for each seismic intensity range, the probability of an RCCS break was determined; the results are shown in Table IV. For example, the median of the RCCS fragility is at a peak ground acceleration of 2.0g. Therefore, for the seismic intensity range of 0.8 – 2.0g, the probability of RCCS break is 50%, which is assumed to be distributed equally between break locations 1 and 2. The area of the duct wall breach was considered a parameter uncertainty, as will be described in Section II.D.

TABLE III. RCCS Fragility (Ref. 7).

System	Percentile	Peak Ground Acceleration (g)		
		5 th	50 th	95 th
RCCS		1.3	2.0	3.0

TABLE IV. RCCS Air Break Top Event Probability.

RCCS Air Break Top Event	Probability
0.06 – 0.2g	
No Break	0.9990
Break Location 1	0.0005
Break Location 2	0.0005
0.2g – 0.4g	
No Break	0.9950
Break Location 1	0.0025
Break Location 2	0.0025
0.4 – 0.8g	
No Break	0.990
Break Location 1	0.005
Break Location 2	0.005
0.8 – 2.0g	
No Break	0.50
Break Location 1	0.25
Break Location 2	0.25

II.B.7. Top Event: Sump Backup

The next top event considers a backup of the RCCS sump system. The sump removes water that enters the RCCS area around the reactor vessel through the use of a sump pump. If a tsunami were to impact the reactor site, it is possible the water may backflow through the sump system and enter the RCCS. While the use of a check valve within the system to prevent backflow is likely, the pressure head of surface flooding (the sump is likely to be located approximately 30m below grade) coupled with the pressure force of the tsunami wave action may cause check valve failure.

As with the probability of a break in the RCCS, the probability of sump backup is varied with seismic intensity range. Similar to the assumption that tsunamis are less likely at lower seismic intensity ranges, the force/impact of the wave action is also assumed to be less severe, and sump backup less likely, with decreasing earthquake intensity. The probabilities for sump backup are shown in Table V. These values are partially based on the fragility of auxiliary systems at the reactor site

(taken from the HTGR PRA (Ref. 7)), which are less robust in general than the RCCS, and modified to also include the increasing probability of a tsunami with higher seismic intensity range¹.

TABLE V. Sump Backup Top Event Probability.

Sump Backup Top Event	Probability
0.06 – 0.2g	
No Sump Backup	0.999
Sump Backup	0.001
0.2g – 0.4g	
No Sump Backup	0.995
Sump Backup	0.005
0.4 – 0.8g	
No Sump Backup	0.99
Sump Backup	0.01
0.8 – 2.0g	
No Sump Backup	0.75
Sump Backup	0.25

II.B.8. Top Event: Sump Restore

For those event sequences that incur a sump backup, the possibility of sump restoration is also considered. The restoration could occur for several reasons. First, after the tsunami has subsided, the pressure on the sump system may lessen, allowing some water to drain from the RCCS and the check valve to operate properly. Secondly, the use of FLEX equipment or other active means may be utilized to remove water from the RCCS. Both situations are combined for the sump restoration top event.

Again, the probability of sump restoration varies with seismic intensity range, as shown in Table VI. As the intensity of the earthquake increases, probability of sump restoration decreases. The timing of sump restoration (if it occurs) was also considered uncertain, and is one of the sampled parameter uncertainties discussed in Section II.D. For the demonstration analysis, the restoration probabilities are derived using engineering judgment. With a complete plant design, the availability of FLEX equipment and the specific design of the sump system could be used to develop more accurate probabilities.

TABLE VI. Sump Restore Top Event Probability.

Sump Restore Top Event	Probability
0.06 – 0.2g	
No Sump Restore	0.01
Sump Restore ¹	0.99
0.2g – 0.4g	
No Sump Restore	0.05
Sump Restore ¹	0.95
0.4 – 0.8g	
No Sump Restore	0.25
Sump Restore ¹	0.75
0.8 – 2.0g	
No Sump Restore	0.5
Sump Restore ¹	0.5

¹ Time of restoration is considered a parameter uncertainty and discussed in Section II.D.

II.B.9. Top Event: Delayed Active Heat Removal

The possibility of the restoration of active heat removal at some period after the earthquake is considered. The probability of active heat removal restoration varies with seismic intensity range, as shown in Table VII, with decreasing possibility as earthquake intensity increases. As with sump restoration, the probabilities are derived using engineering

¹ A tsunami may still be possible for earthquakes in the low seismic intensity range categories, as a powerful earthquake may have occurred at a distance far from the plant (resulting in minimal ground acceleration at the site) but creating a large tsunami that then impacted the reactor site.

judgment, but with a complete plant design and more knowledge of available FLEX equipment, it would be possible to revise the probabilities. Also, the exact time of active heat removal restoration was considered uncertain and sampled as a parameter uncertainty, as will be discussed in Section II.D.

TABLE VII. Active Heat Removal Top Event Probability.

Active Heat Removal Top Event	Probability
0.06 – 0.2g	
AHR Restore ¹	0.9
No AHR Restore	0.1
0.2g – 0.4g	
AHR Restore ¹	0.8
No AHR Restore	0.2
0.4 – 0.8g	
AHR Restore ¹	0.7
No AHR Restore	0.3
0.8 – 2.0g	
AHR Restore ¹	0.25
No AHR Restore	0.75

¹ Time of restoration is considered a parameter uncertainty and discussed in Section II.D.

II.B.10. Success/Failure Criteria

For the passive system to be successful, it must maintain the core/sodium temperature at an acceptable level for 72 hours. This time period was chosen based on NRC rulemaking regarding the establishment of coping time for passive reactor designs. As stated in the standard review plan (NUREG-0800) (Ref. 9), “Because passive plants will not have emergency AC power sources, applicants for such plants need not evaluate station blackout coping duration as long as they are able to demonstrate that the design selected is capable of performing safety-related functions for 72 hours. The 72 hour approach is consistent with the duration approved by the NRC staff for the AP 1000 design.” While this requirement is stated for light-water reactors, the small SFR under consideration here is similar in that it is a passive plant with no emergency AC power sources. However, it is worth noting that during the licensing process of an SFR in the future, this requirement would likely be reevaluated in the context of the plant’s proposed safety systems and inherent characteristics, such as the thermal capacity of the primary sodium pool.

Two metrics are used to assess the status of the core. First, sodium boiling within the core is almost certainly an indication that fuel damage will occur. Second, while the metal fuel used in this SFR design has beneficial reactivity feedback and inherent safety features, fuel-cladding eutectic formation, or the combination of several materials that results in a lower melting point than the individual materials alone, can weaken the cladding at temperatures of about 200°C above normal operating temperatures if exposed for prolonged periods. This topic, and how it is assessed for this scenario, is described in more detail in Section II.F.

II.C. System Modeling

An integrated RELAP5-3D (Ref. 10) model was developed, which explicitly models both the SFR and the RCCS, was utilized for the earthquake/tsunami analysis. The coupled treatment of the reactor system and RCCS is vital to properly assessing the formation of natural circulation flows within the primary sodium system and within the RCCS as it allows for the examination of feedback effects between the primary and heat rejection systems.

A simplified nodalization diagram of the RELAP5-3D model of the SFR is shown in Figure 6. The reactor model includes four primary EM pumps, which pump sodium from the cold pool into the inlet plenum before entering the core region. After leaving the core region, the sodium enters the hot pool before passing through the IHX and back into the cold pool. During scenarios where the normal heat removal pathway through the secondary/intermediate side is lost, heat removal through the reactor vessel walls to the RCCS will result in the development of natural circulation.

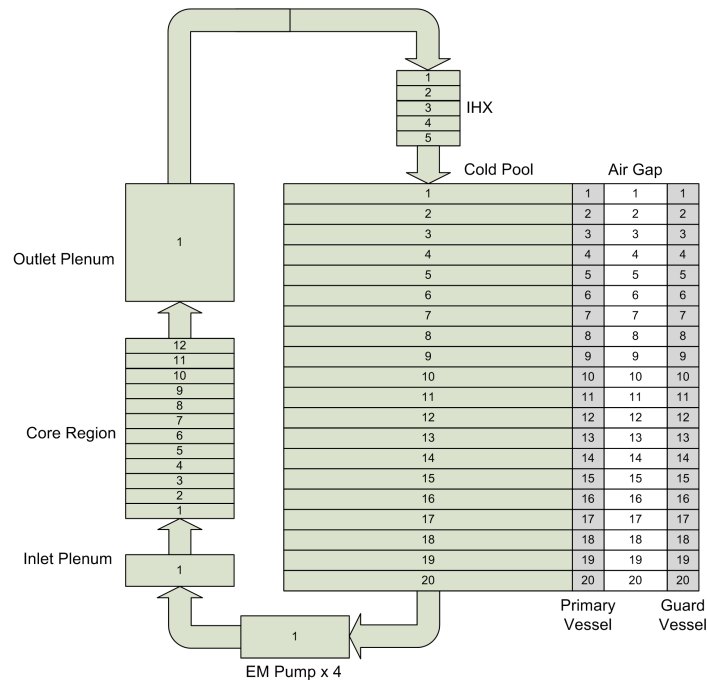


Fig. 6. Simplified Nodalization Diagram of the Primary System of the SFR RELAP5-3D Model².

The RELAP5-3D RCCS model, of which a nodalization diagram is shown in Figure 7, is from previous GA-MHTGR analyses (Ref. 11), with modifications to account for the size difference between the GA-MHTGR vessel and the SFR guard vessel. As discussed in Section II.B, damage to the RCCS was considered in this analysis. Two separate break paths between the hot and cold ductwork of the RCCS were simulated. While the nodalization diagram of the RCCS shows the hot and cold ductwork of the RCCS as separate, in reality there are sections of the ductwork where they are directly adjacent to one another and other sections where the hot ductwork is located inside of the cold ductwork. If a duct wall break were to occur in these areas, a flow path would be created that would allow air to bypass normal pathways and instead flow directly from the cold ductwork into the hot ductwork. The two locations where duct wall breaks were modeled as part of this analysis are shown in Figure 7. The first break path modeled created a flow path from node 409 of the cold ductwork to node 709 of the hot ductwork (referenced in the event tree in Figure 4 as location 1). The second break path modeled created a flow path from node 575 of the cold ductwork to node 706 of the hot ductwork (referenced in the event tree in Figure 4 as location 2). These locations were selected based on previous RCCS analysis of possible break locations between the cold and hot ductwork of the RCCS (Ref. 5). It is important to note that for the current analysis only one break was assumed to occur per scenario, such that either a break was assumed to occur at location 1 OR location 2 OR not at all. The area of the break at each location was treated as an uncertain parameter in each simulation and the treatment of this uncertainty is described in Section II.D.

Water entry into the RCCS from sump backup was also considered in the analysis. To be conservative, the amount of water flooding into the RCCS was assumed to only fill up the lower plenum of the RCCS and not enter into the hot riser ducts. If water were to enter the hot riser ducts, the heat rejection of the RCCS would be enhanced instead of reduced. By filling the lower plenum, the water blocks the air flow pathway between the cold downcomer and the hot riser ducts. To mimic this behavior in the RELAP5-3D model, a valve was added to the model in the cold ductwork path that could be closed to simulate the airflow blockage that the water would cause; the valve could also be re-opened to simulate the restoration of sump operation. This enabled modeling “flooding” of the RCCS without significantly increasing the time each RELAP5-3D simulation required (due to code instabilities with dynamic water movement in the RCCS) which allowed for a large number of simulations to be performed. To simplify the analysis, no partial flooding scenarios were considered. That is, the airflow path from the cold ductwork into the hot riser ducts was either blocked (flooded) or unblocked (not flooded).

² This diagram depicts the flowpath and structures associated with the SFR RELAP5-3D model, but does not accurately represent component locations and elevations.

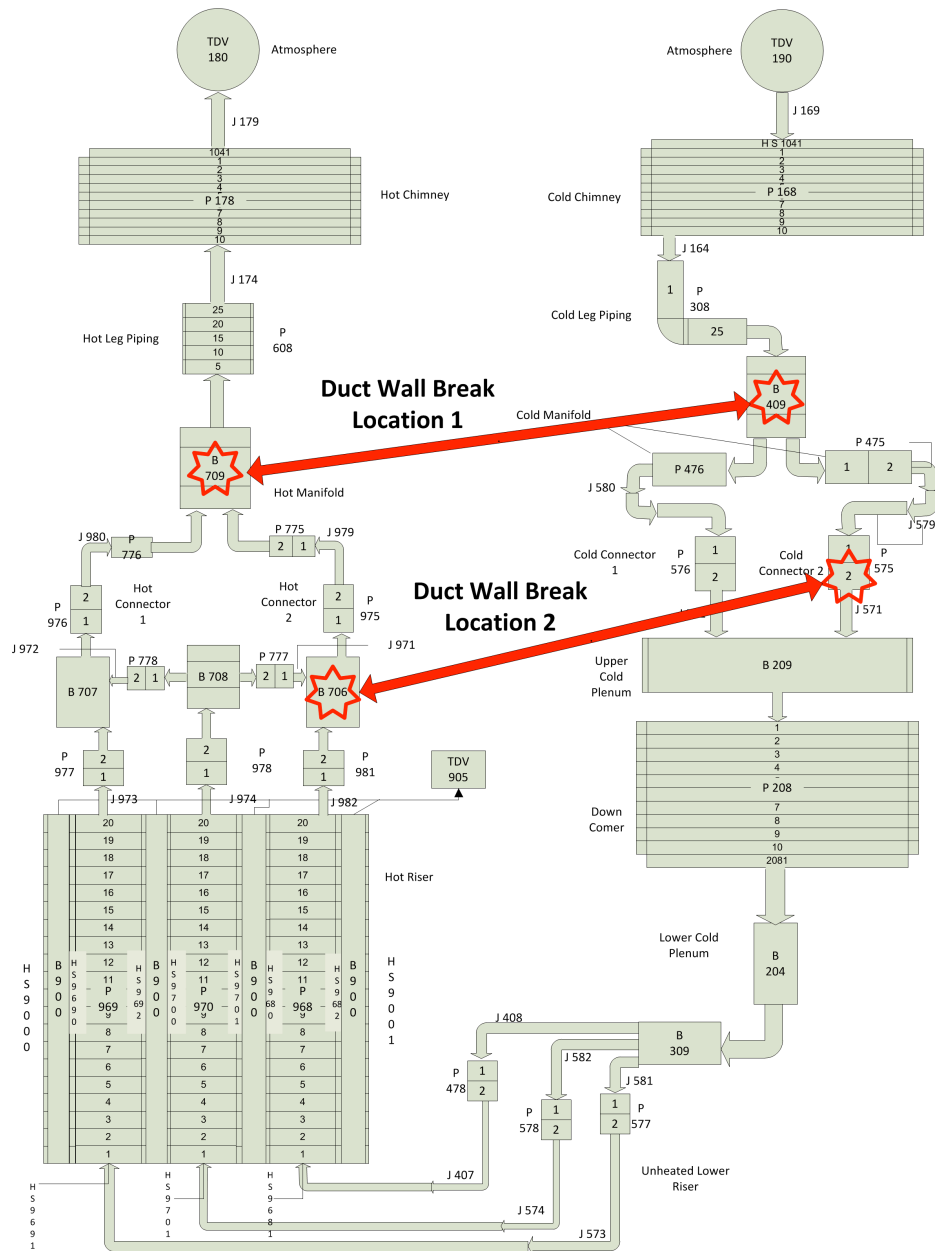


Fig. 7. Nodalization Diagram of the RCCS RELAP5-3D Model with Duct Wall Break Locations.

II.D. Parameter Identification and Uncertainty Quantification

The next step of the analysis was to identify the relevant parameters and associated uncertainties. For this demonstration problem, parameters affecting both the reactor and the RCCS have been selected. An FMEA and HAZOP analysis were previously conducted to identify the important phenomena affecting the performance of the RCCS (Ref. 3). Many of the same uncertainties associated with the reactor and the RCCS in (Ref. 3) were applicable to this external event analysis. In addition to the previously identified uncertain parameters, additional uncertainties, such as RCCS duct wall break area and the time of sump restoration were added. The timing of active heat removal activation was also a source of uncertainty in (Ref. 3), but is treated differently in this analysis, as it is dependent on the magnitude of the earthquake.

Table VIII presents the parameter uncertainties and their distributions/ranges. As the table shows, many uncertainties are the same as previous analysis reported in (Ref. 3), including material properties of the primary vessel, guard vessel, hot riser ducts, steel liner and ducts, ambient air temperature, reactor power level at the time of the initiating event, and decay heat generation during the protected scenarios.

Three new or modified parameter uncertainties (with respect to those used in (Ref. 3)) were considered during this analysis. The uncertainty associated with the duct wall break area was characterized by a uniform distribution with a lower bound of 0.5 m² and an upper bound of 5.50 m². These bounding values were taken from previous analysis of the RCCS (Ref. 5)³.

The uncertainty associated with the time to restore normal sump operation was characterized by a uniform distribution with a lower bound of 1.0 hour and an upper bound of 24.0 hours. These bounding values were based on engineering judgment, but with the assumption that sump restoration due to receding flood waters would occur after one hour, and that restoration due to FLEX equipment was likely to occur within the first day.

As stated previously, the time at which active heat removal capabilities were restored was dependent on the magnitude of the earthquake in the scenario being analyzed. The uncertainty associated with the activation time was treated using uniform distributions except in the case of the highest magnitude earthquake where it was assumed that active power heat removal was activated at 48 hours or was it not activated at all within the first 72 hours following the initiating event. For the other three earthquake intensity ranges, as the intensity of the earthquake increased, so did the minimum time at which active power would be recovered. This assumes that the higher the intensity of the earthquake, the more damaged the infrastructure required for active systems would be, which would lead to increased recovery times.

TABLE VIII. Quantified Uncertainties Considered in the Event Tree Analysis.

Uncertainty	Characterization	Comment
Ambient temperature	U(-30.0, 45.0)	Assume conservative bounds, °C.
Primary vessel emissivity	N(0.77, 0.035)	Mean and bounding percentiles from (Ref. 8).
Primary vessel thermal conductivity	N(1.0, 0.0125)	Scaling factor, assume limits are ±2.5% of mean.
Guard vessel emissivity	N(0.77, 0.035)	Mean and bounding percentiles from (Ref. 8).
Guard vessel thermal conductivity	N(1.0, 0.0125)	Scaling factor, assume limits are ±2.5% of mean.
Hot riser duct emissivity	N(0.77, 0.035)	Mean and bounding percentiles from (Ref. 8).
Hot riser duct thermal conductivity	N(1.0, 0.0125)	Scaling factor, assume limits are ±2.5% of mean.
Steel liner emissivity	N(0.77, 0.035)	Mean and bounding percentiles from (Ref. 8).
Duct surface roughness	lnN(3.45, 0.70)	Large range of uncertainty due to weathering, μm.
Initial power level	N(1.0, 0.025)	Scaling factor, limits are ±5% of mean.
Decay heat curve	N(1.0, 0.025)	Scaling factor, limits are ±5% of mean.
RCCS Break Area	U(0.5, 5.50)	Breach size, m ²
Sump Restore	U(1.0,24.0)	Time, hours
Active heat removal activation time		Time, hours
0.06 – 0.2g		
Activation time	U(6.0, 12.0)	
0.2 – 0.4g		
Activation time	U(12.0, 24.0)	
0.4 – 0.8g		
Activation time	U(18.0, 36.0)	
0.8 – 2.0g		
Activation time	Only 48	

II.E. Sensitivity Analysis and Screening

The following step of the analysis procedure was to perform sensitivity analyses of the selected variables and screen out parameters and uncertainties that were not expected to significantly affect scenario progression and system behavior. These sensitivity analyses were carried out using RELAP5-3D. Several modeling uncertainties were previously investigated during the analysis reported in (Ref. 3). Most of these uncertainties, with the exception of the inherent reactivity feedback, were treated similarly in this analysis. The uncertainty associated with inherent reactivity feedbacks were not considered as part of this analysis because only protected scenarios were considered.

The effect of pump coastdown failure on scenario progression was investigated as part of this analysis. As demonstrated in (Ref. 3), unprotected scenarios that include multiple pump coastdown failures may possibly result in core damage due to high power to flow ratios. For this analysis, a variety of sequences from the earthquake event tree were simulated with a varying number of pump coastdown failures from zero to four out of a possible four. The results demonstrated negligible differences in the sequences (less than a 5°C change in peak cladding temperature from no pump coastdown failures to four pump coastdown failures for the same sequences). This result was also seen in the PRISM PRA (Ref. 8), where pump

³ Since the RELAP5-3D RCCS model has two identical RCCS loops, it was assumed that an identical break, or half the total break area, occurred in each of the RCCS loops.

coastdown failure has negligible effects for protected scenarios. The elimination of pump coastdown failures from the earthquake event tree reduced the number of sequences from 360 to 72 and greatly reduced the computational time needed for uncertainty propagation.

All of the parameter uncertainties shown in Table VIII were propagated as part of this analysis, as the number of uncertainties was not considered overly burdensome. In a realistic analysis, the uncertainties under consideration may number into the hundreds. In this case, further sensitivity and screening analyses would help reduce this to a manageable number.

II.F. Propagation of Uncertainties

Unlike the analysis in (Ref. 3), which compared both a mechanistic and simulation-based approach to the propagation of uncertainties and integration into the PRA, this analysis focused on combining the two methods based on lessons learned from (Ref. 3) and interactions with industry. Initial feedback of the previous analysis by industry indicated a reluctance to transition to a completely simulation-based PRA structure, as the methods are still relatively immature. In the previous analysis, it was shown that there is generally little difference between the mechanistic and simulation-based methods for scenarios where there are few “logic-based” uncertainties (such as the operator action considered in (Ref. 3)). Instead, many parameter uncertainties can be handled through direct uncertainty propagation, as long as simulation run-times are not extremely cost-prohibitive. Therefore, for this analysis, uncertainties related to dynamic variables, such as sump or active heat removal recovery, were directly propagated through sampling as inputs, rather than as branch conditions for a simulation-based method.

For the combined uncertainty propagation methodology, 100 RELAP5-3D simulations were performed for each sequence of the earthquake event tree seen in Figure 4. The parameter uncertainty values were chosen through Monte Carlo sampling, with no variance reduction techniques employed (this was done as a condition of the statistical method to calculate confidence intervals for the results, discussed below). Each RELAP5-3D returned a peak cladding temperature and a binary sodium boiling metric (Y/N). The same core damage probability formula used in (Ref. 3), which based the probability of core damage on sodium boiling and a conservative eutectic penetration formula, was used for this analysis. While it now appears that the core damage probability formulation is likely overly conservative with regards to eutectic penetration, the same formula was used to allow for the comparison of the results of previous and current analyses.

II.G. Results

The results of the earthquake event tree analysis are shown in Table IX. The mean core damage frequency (CDF) is presented along with a 95% confidence interval result. Again, the 95% confidence value used is not conservative with respect to the parameter uncertainties; however, it provides information related to the statistical accuracy associated with the number of simulations conducted. In this way, the change in statistical confidence from conducting more/less simulations can be accounted for in the final results. More detail on this statistical calculation can be found in (Ref. 12).

Unlike the previous analysis results in (Ref. 3), there is little difference in the CDF results using the eutectic penetration and sodium boiling metric, or just using sodium boiling alone. What this implies is that for the risk dominant sequences (the sequences that are the biggest contributor to the overall CDF) sodium boiling occurs regardless of the input uncertainties and not just high peak cladding temperatures. Also, the relatively small variation between the mean value and the 95% confidence interval value also signals that the choice of 100 simulations per sequence to characterize the parameter uncertainty space is likely sufficient, and there appears to be no drastic change in outcome (for risk dominant sequences) across the uncertainty space.

The results of this analysis show that the risk dominant sequences occur as part of the largest seismic intensity range (0.8 – 2.0g) despite the lower frequency of the event occurring. This is due to the high probability of RCCS break and sump backup, coupled with the lower probability of sump and active heat removal restoration. These factors outweigh the reduction in probability caused by the rarity of the event. However, it should be noted that the probabilities related to these events are also those that were the most heavily based on engineering judgment, due to a lack of a completed plant design.

TABLE IX. Earthquake/Tsunami Event Tree Final Results.

Core Damage Metric	Mean CDF (/yr)	CDF - 95% Confidence Interval (/yr)
Sodium Boiling and Simple Eutectic Penetration Model	1.28×10^{-6}	1.32×10^{-6}
Sodium Boiling Only	1.26×10^{-6}	1.30×10^{-6}

II.H. Result Analysis

A series of correlation analyses were performed to examine the influence of the parameter uncertainties shown in Table VIII. Three different correlation measures, shown in Table X, were used for this analysis to capture the variety of possible correlation types. Pearson is used as a measure of linear correlation between two variables. However, since Pearson can struggle with nonlinearity or non-normal variables (as is the case here), both Kendall and Spearman correlation coefficients are also utilized to give insight into non-linear correlations through the use of variable rank. Kendall is used in conjunction with the more popular Spearman coefficient, as the Kendall rank correlation coefficient is often time more accurate at smaller sample sizes. As always, it is important to note that correlation does not imply causation, but can often times provide insight into system performance.

TABLE X. Correlation Descriptions.

Correlation	Description
Kendall	Non-parametric rank correlation
Spearman	Non-parametric rank correlation
Pearson	Linear correlation measurement

The sequences of the earthquake event tree in Figure 4 were grouped based on similar properties for the correlation analysis. The correlation results for sequences of the event tree where no RCCS break occurred are provided in Figure 8. As can be seen from the results, the initial reactor power level, the decay heat curve, and the sump restoration time (if sump backup occurred) were the most influential variables on the peak cladding temperature. The results are fairly consistent across all three correlation types. Of the material properties, the reactor (primary) vessel thermal conductivity appears to be the most influential, followed closely by the reactor vessel and guard vessel emissivities.

The correlation results for event tree sequences with RCCS breaks for location 1 and for location 2 can also be found in Figure 8. As with the sequences with no RCCS breaks, the main influential parameters are the initial reactor power level, the decay heat curve, and the sump restoration time (if sump backup occurred). Surprisingly, the effect of the size break appears to be very minor for location 1, with only a slightly larger influence for location 2, which implies that occurrence of the break is more important than the size of the break for the range of break sizes considered in this analysis.

Lastly, the correlation results for sequences with sump backup and sump restoration are provided in Figure 8. As the results show, the time of sump restoration is vastly important to the final peak cladding temperatures, with a correlation value approaching one (implying perfect correlation) across all three metrics. This aligns with what would be expected, as sump backup causes a complete blockage of RCCS flow, and the time of flow restoration is pivotal to the restoration of heat removal from the primary system.

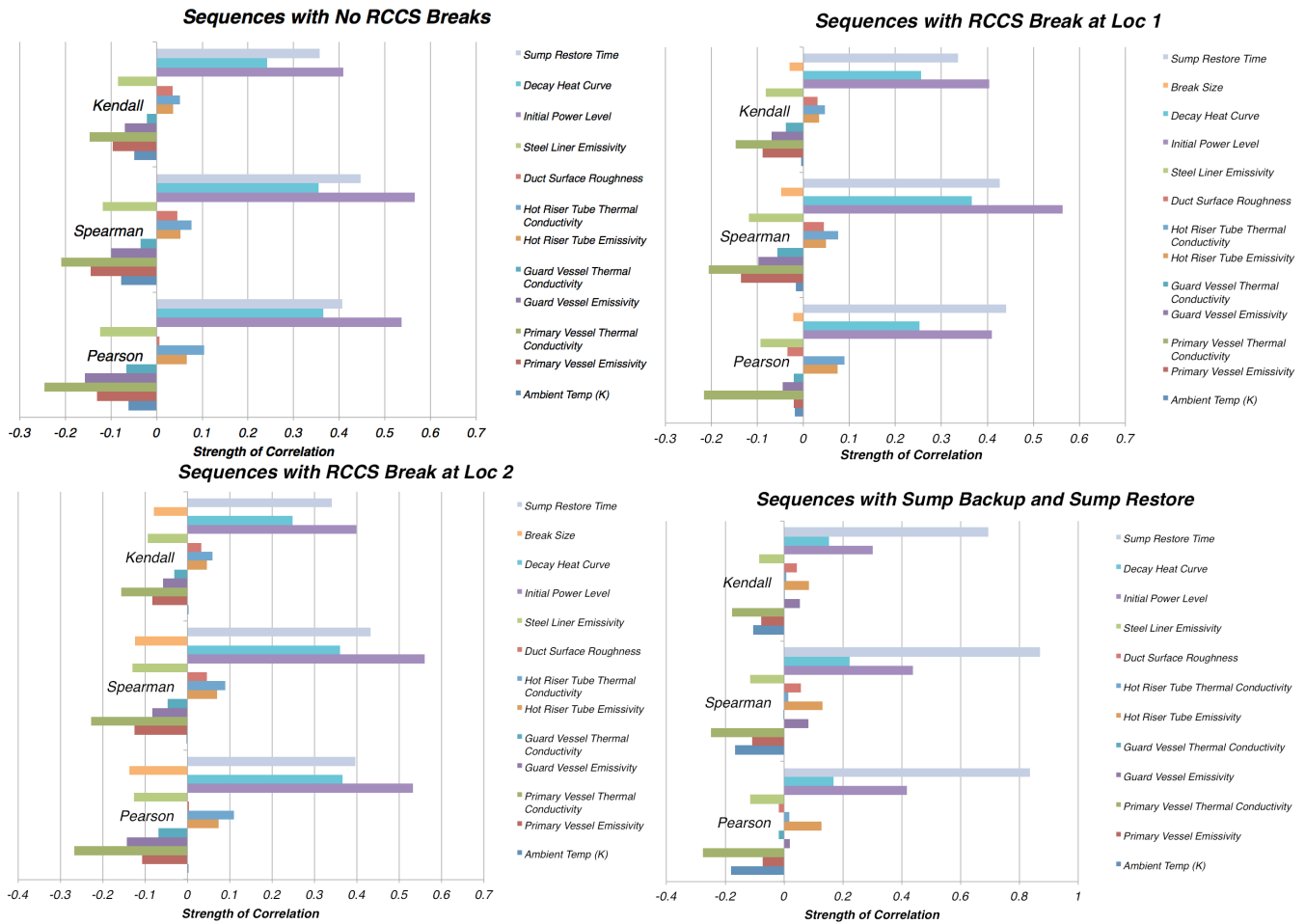


Fig. 8. Correlation Results.

III. CONCLUSIONS

The current analysis detailed one methodology for the assessment of passive system reliability during an extreme external event within a probabilistic framework. A hybrid approach, in which elements from a simulation-based methodology were integrated into a conventional mechanistic framework, was adopted for the analysis of RCCS performance in degraded and damaged states caused by an earthquake and subsequent tsunamis. This hybrid approach exhibited good compatibility with the goals of the passive system demonstration problem, and was able to address the challenges typically presented by passive system reliability assessments.

The hybrid analysis methodology allowed for the treatment of uncertainties within the top events of the event tree and through Monte Carlo sampling of parameter uncertainties. By delineating the treatment of uncertainties in this fashion, the dependence on simulation-based code branching conditions was removed, which was seen as a potential hurdle by industry commenters following previous analysis (Ref. 3). However, if the scenario were to include many more dynamic variables, such as the inclusion of many possible operator actions or possibly human error pathways, simulation-based code branching may still be the most favorable approach, as the size of the hybrid approach methodology may become difficult to manage.

It is important to note that many aspects of this analysis utilized engineering judgment in the absence of actual design and operating data, where many of the assumptions in this analysis were largely conservative. As a consequence, it can be concluded that the reliability results presented here are very conservative and do not necessarily represent best-estimate data. Additionally, this analysis is not intended to be a commentary on the viability of coupling of an SFR with the RCCS; these systems were chosen only for demonstration purposes, and many simplifying assumptions were made. The primary conclusion of this effort should not be the quantified reliability or failure results, but rather should be regarding the viability of the demonstration methodologies for passive systems.

ACKNOWLEDGMENTS

Argonne National Laboratory's work was supported by the U.S. Department of Energy, Assistant Secretary for Nuclear Energy, Office of Nuclear Energy, under contract DE-AC02-06CH11357.

REFERENCES

1. G. APOSTOLAKIS, et al., "A Proposed Risk Management Regulatory Framework," NUREG-2150, U.S. Nuclear Regulatory Commission, (2012).
2. M. MARQUES, et al., "Methodology for the Reliability Evaluation of a Passive System and its Integration into a Probabilistic Safety Assessment," Nuclear Engineering and Design, vol. 235, pp. 2612-2631, (2005).
3. A. BRUNETT, M. BUCKNOR, and D. GRABASKAS, "A Passive System Reliability Analysis for a Station Blackout," Proceedings of ICAPP 2015, Nice, France, May 3-6, (2015).
4. U.S. Department of Energy, "Preliminary Safety Information Document for the Standard MHTGR," HTGR-86-024, Vol. 1, Amendment 13, (1992).
5. U.S. Department of Energy, "Preliminary Safety Information Document for the Standard MHTGR," HTGR-86-024, (1986).
6. Idaho National Laboratory, "Systems Analysis Programs for Hands-on Integrated Reliability Evaluations (SAPHIRE) Version 8: User's Guide," (2011).
7. U.S. Department of Energy, "Probabilistic Risk Assessment for the Standard Modular High Temperature Gas-Cooled Reactor," DOE-HTGR-86-011, (1987).
8. General Electric, "PRISM Preliminary Safety Information Document," GEFR-00793, UC-87Ta, San Jose, CA, (1987).
9. U.S. Nuclear Regulatory Commission, "Standard Review Plan for the Review of Safety Analysis Reports for Nuclear Power Plants: LWR Edition," NUREG-0800 Revised, (2010).
10. The RELAP5-3D Code Development Team, "RELAP5-3D Code Manual," Idaho National Laboratory, Idaho Falls, ID, INEEL-EXT-98-00834, Rev. 4, (2012).
11. S. LOMPERSKI, et al., "Air-Cooled Option RCCS Studies and NSTF Preparation," ANL-GenIV-179, (2011).
12. D. GRABASKAS, M. BUCKNOR, A. BRUNETT, and M. NAKAYAMA, "Quantifying Safety Margin Using the Risk-Informed Safety Margin Characterization (RISMC)," Proceedings of PSA 2015, Sun Valley, ID, April 26-30, (2015).